Proceedings of the 20th International Conference on Soil Mechanics and Geotechnical Engineering– Rahman and Jaksa (Eds)

Thermal and chemical effects on buffer materials in a rad-waste disposal repository: experiments and numerical simulation by a double-structure hypoplasticity model

Effets thermiques et chimiques sur les matériaux tampons d'un stockage de déchets radiques: expériences et simulation numérique par un modèle hypoplastique à double structure

Fuchen Teng & Yong-Cheng Sie

Department of Civil and Construction Engineering, National Taiwan University of Science and Technology, Taiwan, fteng@mail.ntust.edu.tw

Chihping Kuo

Department of Civil Engineering and Environmental Resources Management, Minghsin University of Science and Technology Affiliation, Taiwan

Chung-Ren Huang

Center of civil Engineering and architecture, Sinotech Engineering Consultants Ltd., Taiwan

Biing-Shzou Hwang

Department of nuclear backend management, Taiwan Power Company, Taiwan

ABSTRACT: A series of one-dimensional swelling experiments on pure bentonite specimens were conducted to investigate the thermal and chemical effects on the swelling potential of bentonites. Thermal conditions, varying from 25°C to -5°C, were controlled. Both de-ionized water and artificial sea water were employed as the saturation solution for specimens during multiple wetting-drying cycles. Experimental results revealed that the low temperature and ions in solutions degrade the swelling potential of buffer materials, especially the specimen with a lower density. The cracking pattern during the drying process were strongly influenced by the saturation solution which affected the specimen integrity. To reasonably reproduce the complex behavior and high swelling potential of buffer materials, an advance constitutive model, double-structure hypoplasticity model for clays (DSHC), capable of modelling the thermal-hydraulic-mechanical coupled effects, was used in this study. A series of parametric study was conducted to investigate the sensitivity and influence of important parameters. The thermal and chemical effect was then studied through the DSHC model in an element test driver.

RÉSUMÉ : Une série d'expériences de gonflement unidimensionnel sur des spécimens de bentonite pure ont été menées pour étudier les effets thermiques et chimiques sur le potentiel de gonflement de la bentonite. Les conditions thermiques, variant de 25°C à -5°C, ont été contrôlées. De l'eau désionisée et de l'eau de mer artificielle ont été utilisées comme solution de saturation pour les spécimens pendant plusieurs cycles de séchage-mouillage. Les résultats expérimentaux ont révélé que la basse température et les ions dans les solutions dégradent le potentiel de gonflement des matériaux tampons, en particulier l'échantillon avec une densité plus faible. Le motif de fissuration pendant le processus de séchage a été fortement influencé par la solution de saturation qui a affecté l'intégrité de l'échantillon. Pour reproduire raisonnablement le comportement complexe et le potentiel de gonflement élevé des matériaux tampons, un modèle constitutif avancé, un modèle hypoplasique à double structure pour les argiles (DSHC), capable de modéliser les effets couplés thermique-hydraulique-mécanique, a été utilisé dans cette étude. Une série d'études paramétriques a été menée pour étudier la sensibilité et l'influence de paramètres importants. L'effet thermique et chimique a ensuite été étudié à l'aide du modèle DSHC dans un pilote de test d'éléments.

KEYWORDS: bentonite, THM, double structure, hypoplasticity model

1 INTRODUCTION

Underground disposal with the concept of multi-barriers is employed for the final disposal of low-level radioactive waste (LLRW). The multi-barrier system considered both engineering and natural barriers including solidified waste, container, buffer, backfill, engineering barrier, and host rock. The buffer and backfilling materials shall have low permeability and high adsorbability to retard the migration of radioactive nuclide.

Buffer materials (bentonite materials) with high swelling potential are used in low-level radioactive waste (radwatse) disposal facility to confined and retard the radionuclide for hundreds to thousands of years. Thermal and chemical environments may subject to change during the disposal period and thus affects the performance of buffer materials. Thus, the influence of geo-environmental change should be carefully investigated to ensure the performance of bentonite material in a rad-waste disposal repository. In this study, a series of one-dimensional swelling experiments on pure bentonite specimens were conducted to investigate the thermal and chemical effects on swelling potential. Thermal conditions, varying from 25°C to -5°C, were controlled via a temperature chamber. Both de-ionized water and artificial sea water were employed as the saturation solution for specimens during multiple wetting-drying cycles. To reasonably reproduce the complex behavior and high swelling potential of buffer materials, an advance constitutive model, double-structure hypoplasticity model for clays (DSHC), capable of modelling the thermal-hydraulic-mechanical coupled effects, was used in this study. A series of parametric study was conducted to investigate the sensitivity and influence of important parameters. The thermal and chemical effect was then studied through the DSHC model in an element test driver.

2 TEST MATERIAL AND TEST PLAN

2.1 *Bentonite material and sample preparation*

Bentonite can be divided into sodium bentonite and calcium bentonite. In general, sodium one has better swelling performance than the calcium one. In this study, a sodium bentonite Kunigel-V1 (KV1) from Japan is chosen as the test material. Kunigel-V1 is widely used in civil engineering applications, especially for the research and development of waste disposal in Japan. The basic properties of KV1 is listed in Table 1. The chemical composition results of KV1 in this study are shown in Table 2. In KV1, the main chemical components are SiO_2 and Al_2O_3, and the composition percentages are 64.44% and 24.53%, respectively. The contents of CaO and Na_2O in bentonite are similar, with CaO being 2.898% and Na_2O being 2.62%.

The bentonite sample is prepared at a water content of 10% with a dimension of 50 mm in radius and 10 mm in thickness. Samples are compacted via a static loading with a velocity of 0.3 mm/min. The designed density for the samples are 1.53, 1.65 and 1.85 g/cm^3. The sample preparation processes are shown in Figure 1.

Table 1. Basic properties of KV1

Property	Value
Nature water content (%)	9.2 ± 0.3
Specific gravity	2.61
Liquid limit (%)	452
Plasticity index	418
Montmorillonite content (%)	62

Table 2. Chemical composition results of KV1

Chemical composition	Percentage (%)
SiO_2	63.441
Al_2O_3	24.527
Fe_2O_3	2.454
CaO	2.898
MgO	2.484
Na_2O	2.620
SO_3	0.656
K_2O	0.354
TiO_2	0.208
BaO	0.200
MnO	0.095
P_2O_5	0.038
ZrO_2	0.013
Cl	0.011

Table 3. Comparison of chemical compositions in artificial seawater

Chemical composition	ASTM D1141	Komine et al. (2009)	ASTM D1141-98 (this study)
NaCl	24.5	24.55	24.53
$MgCl_2$	11.1	11.12	5.2
Na_2SO_4	4.1	4.09	4.09
$CaCl_2$	1.2	1.54	1.16
KCl	0.7	0.69	0.695
NaHCO	-	0.20	0.201

Note: gram per liter artificial sea water

Table 4. Saturation solutions used in drying-wetting cycles

		Solutions in different cycles				
Test	Density (g/cm^3)	1	2	3	4	5
1	1.53	DI	DI	DI	DI	DI
2	1.54	DI	ASW	DI	DI	DI
3	1.53	DI	ASW	ASW	ASW	ASW
4	1.63	DI	DI	DI	DI	DI
5	1.64	DI	ASW	DI	DI	DI
6	1.65	DI	ASW	ASW	ASW	ASW

Figure 1. Bentonite sample preparation

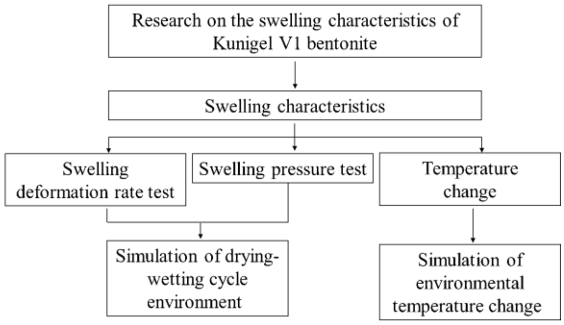

Figure 2. Test plan

2.2 *Saturation solution*

In order to investigate the impact of saturation solution on the swelling potential of bentonite, two solutions were used in this study which are deionized water (DI) and artificial seawater (ASW). The artificial sea water is made by mixing artificial sea salt with a certain proportion of deionized water. The sea salt used in this study is a product that complies with the ASTM D1141-98. Table 3 listed the composition of artificial seawater used in this study and reference.

2.3 *Test plan*

Swelling tests conducted in this study included: swelling deformation test and swelling pressure test. Control factors included different saturation solutions (DI water and artificial sea water), saturation cycles (see Table 4), and environmental temperatures (25°C~-5°C). Detail test plan is shown in Figure 2.

3 TEST RESULTS

3.1 *Impact of saturation solution in wetting-drying cycles*

This section presents the swelling pressure difference between different saturation solutions after wetting-drying cycles. Figures 3 and 4 show the swelling pressure in each cycle for samples with low and high density, respectively. Test results yield that the higher sample density existed a smaller swelling pressure difference, which means the bentonite sample is less affected by the saturation solution type. An index, ratio of maximum swelling pressure (RSP), was introduced to evaluate the ratio of following swelling pressure to that in the second saturation under artificial sea water.

$$RSP = \frac{SP_n}{SP_{2,AW}} \quad (1)$$

where n is the following saturation cycle; SP is the swelling pressure.

Figure 5 & 6 show the RSP for both low and high density samples. For low density bentonite samples, the swelling pressure is easily affected by the saturation solution and yield a different trend when the saturation solution changed. In the contrary, for high density samples, the RSP converged to a consistent level after several wetting cycles. Komine et al. (2009) pointed out that for samples with high dry density or high montmorillonite content with bentonite, the effect of artificial seawater on the swelling characteristics is slight. Thus, the highly compacted bentonite is not easily affected by the chemical components in the saturation solution.

3.2 *Impact of environmental temperature*

This section presents the effect of environmental temperature on the one-dimensional swelling deformation. The temperature is changing from 25℃ to 5℃ for samples with dry density of 1.65 g⁄cm^3, and 25℃ to -5℃ for samples with dry density of 1.85 g⁄cm^3. The temperature variation is used to simulate the unexpected environmental change during the long disposal period.

Figure 7 shows the swelling deformation in both saturation stage and cooling stage. Both samples show a decreasing swelling deformation rate while temperature is decreasing. Table 5 lists the swelling deformation rate under 25℃, 15℃, and 5℃. We can find out that when the temperature drops, the rate has a significant decreasing trend.

Figure 8 shows the welling deformation in both saturation stage and cooling stage, and the temperature will be lowered to −5℃. For temperature higher than 0℃, both samples show a decreasing swelling deformation rate while temperature is decreasing. However, once the temperature becomes negative, a sudden swelling was observed in both samples. Table 6 lists the swelling deformation rate under 25℃, 15℃, 5℃, 0℃ and -5℃.

3.3 *Cracking pattern after wetting-drying cycles*

This section presents the cracking pattern of bentonite samples after 5 wetting-drying cycles with different saturation solutions. Figure 9 shows the photos of six bentonite samples after all wetting-drying cycles, only (c) and (f) are the samples saturated with ASW since the 2nd cycle. For the samples saturated with 5DI or DI-ASW-3DI, that is (a), (b), (d) & (e), the samples showed a collapsed phenomenon which means the sample integrity is affected by the saturation solution. For the sample saturated with DI-4ASW, the samples only cracked on the surface slightly. The salt in the ASW causes a slower evaporation rate in the drying of the sample. The solution with higher salt concentration makes the saturated vapor pressure on the surface lower and reduces the rate of water evaporation. Thus, the samples saturated with ASW will have less evaporation and result in less cracks.

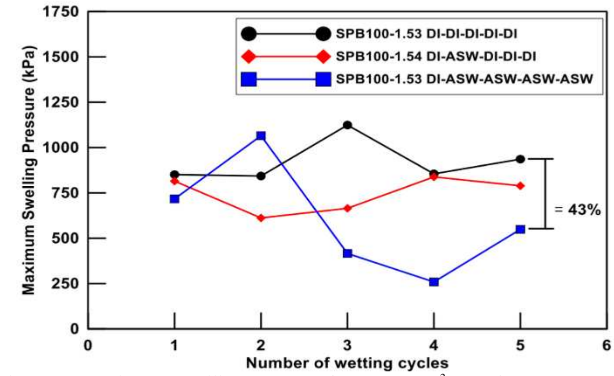

Figure 3. Maximum swelling pressure for 1.54 g⁄cm^3 samples

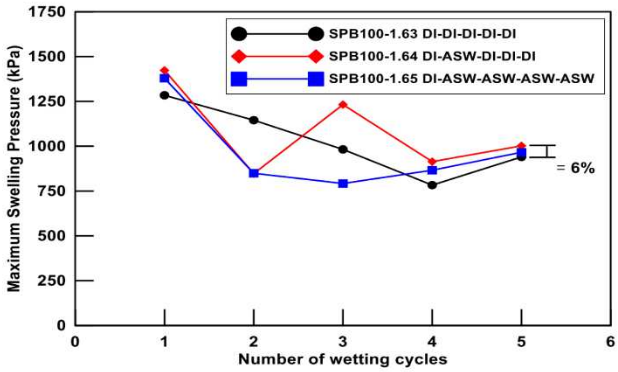

Figure 4. Maximum swelling pressure for 1.64 g⁄cm^3 samples

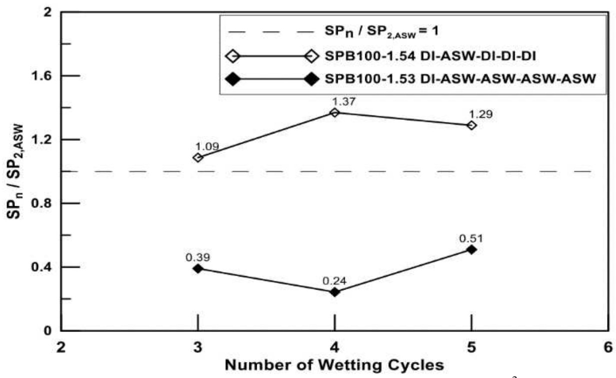

Figure 5. Ratio of maximum swelling pressure for 1.54 g⁄cm^3 samples

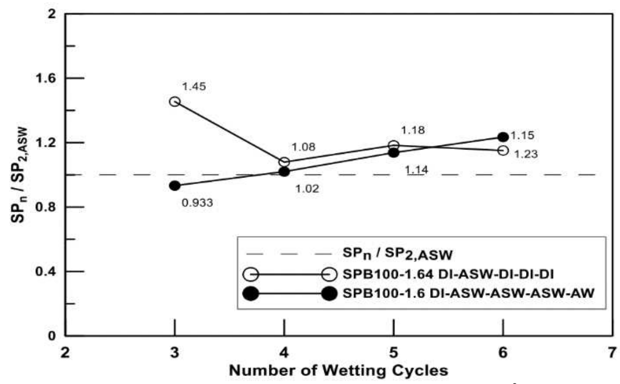

Figure 6. Ratio of maximum swelling pressure for 1.64 g⁄cm^3 samples

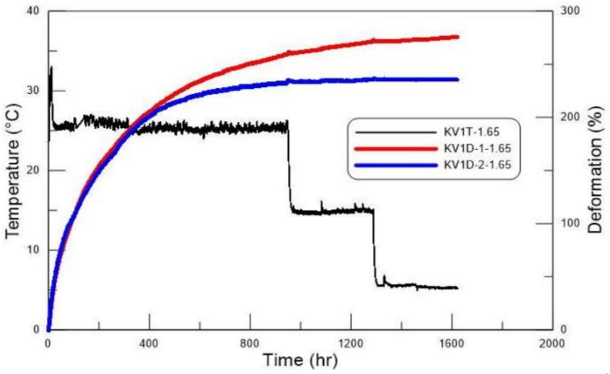

Figure 7. Swelling deformation with varying temperature for 1.65 g/cm³ samples

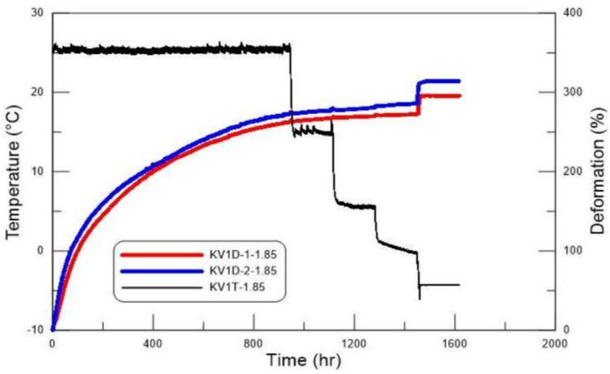

Figure 8. Swelling deformation with varying temperature for 1.85 g/cm³ samples

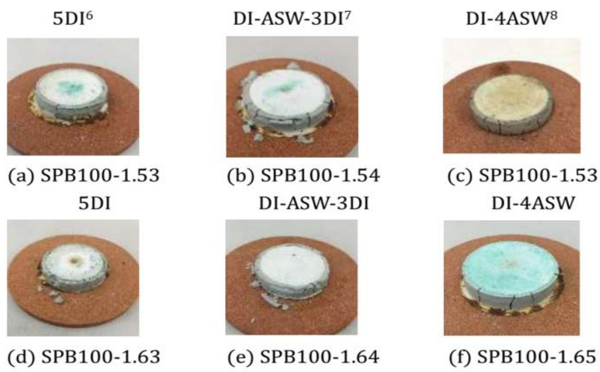

Figure 9. Cracking pattern after final wetting-drying cycle

Table 5. Deformation rate at different temperature for 1.65 g/cm³ sample

Temperature (℃)	KV1DR-1-1.65	KV1DR-2-1.65
25	0.018866%	0.016229%
15	0.009353%	0.003214%
5	0.004921%	0.00005%

Table 6. Deformation rate at different temperature for 1.85 g/cm³ sample

Temperature (℃)	KV1DR-1-1.85	KV1DR-2-1.85
25	0.015644%	0.016132%
15	0.006967%	0.007737%
5	0.003337%	0.005493%
0	0.002508%	0.004647%
-5	0.065~0.000168%	0.07842~0.00243%

Table 7. The parameters for DSHC

Parameters	Description
ϕ_c (°)	Critical state friction angle of macrostructure in a standard soil-mechanics context
λ^*	Slope of isotropic normal compression line in $\ln(p^M/p_r)$versus $\ln(1+e)$space
κ^*	Macrostructural volume strain in p^Munloading
N	Position of isotropic normal compression line in $\ln(p^M/p_r)$ versus $\ln(1+e)$ space
ν	Stiffness in shear
n_s	Dependency of position of isotropic normal compression line on suction
l_s	Dependency of slope of isotropic normal compression line on suction
n_T	Dependency of position of isotropic normal compression line on temperature
l_T	Dependency of slope of isotropic normal compression line on temperature
m	(1) Control of f_u and thus dependency of wetting-/heating-induced compaction on distance from state boundary surface; (2) control of double-structure coupling function and thus response to wetting-drying and heating-cooling cycles (Mašín 2013b)
a_s	Dependency of microstructural volume strains on temperature
k_m	Dependency of microstructural volume strains on p^m
e^m_{r0}	Reference microstructural void ratio for reference temperature T_r, reference suction s_r, and zero total stress
c_{sh}	Value of f_m for compression
$s_{e0}(kPa)$	Air-entry value of suction for reference macrostructural void ratio e^M_0
α	Dependency of macrostructural air-entry value of suction on temperature
b	Dependency of macrostructural air-entry value of suction on temperature
a_e	Ratio of air entry and air expulsion values of suction for macrostructure water retention model
s_r	Reference suction for e^m
e^M_0	Reference macrostructural void ratio for air-entry value of suction of macrostructure
$T_r(K)$	Reference temperature

Table 8. DSHC parameters for KV1

Parameters	DI water	ASW
ϕ_c (°)	25	25
λ^*	0.8286	0.8286
κ^*	0.26358	0.26358
N	11.595	11.595
ν	0.25	0.25
n_s	0.005	0.005
l_s	0.0048	0.0048
m	35	35
k_m	0.09	0.09
$s_r(kPa)$	-80000	-70000
e^m_{r0}	0.12	0.12
$s_{e0}(kPa)$	-15	-10
e^M_0	0.3	0.5
$T_r(K)$	294	294
a_e	1.55	0.75
$p_t(kPa)$	0	0
C_{sh}	0.95	0.05

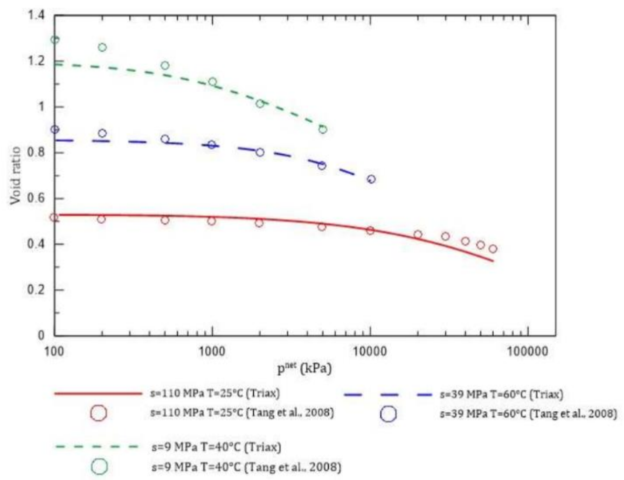

Figure 10. Prediction of swelling characteristic for MX-80 by DSHC model (Masin 2017)

4 NUMERICAL SIMULATION ON BENTONITE SWELLING

To simulated the swelling of bentonite during saturation, an advanced soil constitutive model capable of simulating the high swelling potential is used in this study. The model and simulation unit is introduced below.

4.1 *Soil constitutive model: double-structure hypoplasticity model for clays*

The soil model, double-structure hypoplasticity model for clays (DSHC), used in this study is an advanced T-H-M model developed by Masin (2017). The model is based on the hypoplasticity model for clays (Masin 2005) and combined with double structure concept which can consider the swelling due to micro- and macro- structure in bentonite. Masin (2017) used the DSHC model to simulate the swelling characteristic of MX-80 bentonite under different suction and temperature. The high swelling potential of bentonite can be well predicted by the model, as shown in Figure 10.

4.2 *Simulation on swelling characteristic of bentonite*

An element simulation driver, Triax, developed by Masin (2005) was applied in this study to calibrate the DSHC parameters for KV1. In order to simplified the calibration process, an Auto-Triax program coding by Visual Studio was developed by the authors. Auto-Triax can optimize the chosen parameters within a range based on the test data, that is the swelling pressure of KV1. The parameters for DSHC were listed in Table 7

Five wetting-drying cycles with different saturation solutions were simulated. Simulation results were compared with the test data as shown in Figure 11 and 12. Due to the different saturation solution used, the DSHC model parameter will be adjusted to fit the swelling potential difference. Detail parameters for both simulations are listed in Table 8. In general, the DSHC model with proper parameters can predict the swelling characteristic of KV1 even under different saturation solutions..

5 DISCUSSION AND CONCLUSION

5.1 *Discussion*

Based on the finding in this study and related literature, we found out that the highly compacted bentonite particles have stronger electrostatic interactions repulsive force, thus the spacing between the particles is very small and the net negative potential energy is generated between the particles, which can also be called the negative charge field. The negative charge field is like semi-permeable membranes. The negative charge field repels the anions in the solution that try to pass the bentonite sample. This phenomenon is called Donnan exclusion effect.

In order to keep the electric neutrality in the saturation solution, the cations and anions remain in the solution together, which causes the movement of the cations in the bentonite to be restricted. The overall effect is that the charged ions cannot easily pass through the highly compacted bentonite, while the charged neutral water molecules can travel freely, as shown in Figure 13. For bentonite samples with higher dry density, the electrostatic repulsion of the negative charge field makes it difficult for the cations in the solution to replace with the cations between the crystals. Thus, the swelling pressure is less affected by saturation solutions.

5.2 Co*nclusion*

The swelling characteristic of KV1 bentonite subjected to different saturation solutions and environmental temperature was investigated experimentally in this study. A numerical based on advance soil model was use to simulate the swelling pressure under wetting-drying cycles. Some conclusions can be listed below:

(1) Higher sample density can prevent the saturation solution affecting the swelling potential. The RSP for high density sample is between 1.15-1.23 after the final wetting-drying cycle.
(2) In general, lowering the environmental temperature yields a slower swelling deformation rate; however, once the temperature became negative, a sudden swelling will occur.
(3) In order to reflect the impact of different saturation solution on swelling pressure, the parameters of DSHC model should be adjusted. swelling pressure (RSP), is introduced to evaluate the ratio of following swelling pressure to that in the second saturation under artificial sea water. where n is the following saturation cycle; SP is the swelling pressure.

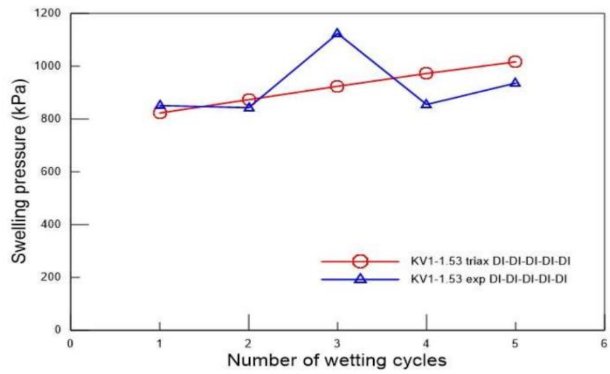

Figure 11. Prediction of swelling pressure under DI water saturation

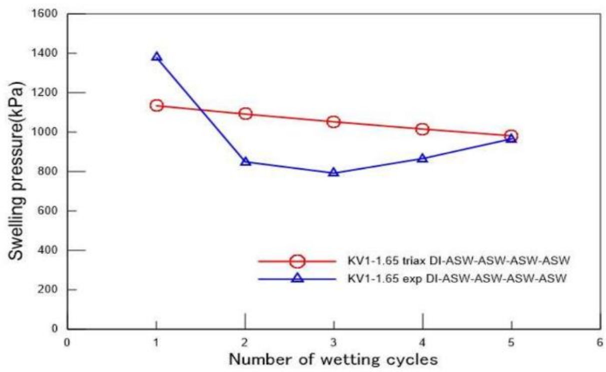

Figure 12. Prediction of swelling pressure under ASW water saturation

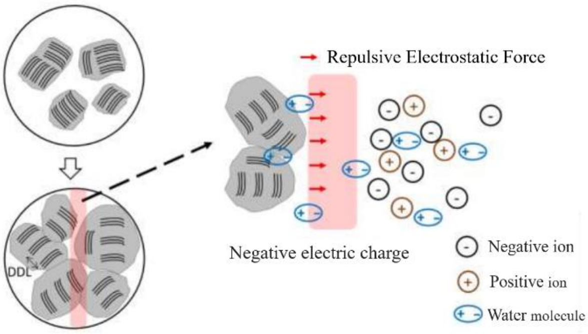

Figure 13. Negative electric charge schematic diagram

6 REFERENCES

Akinwunmi, B., Sun, L., Hirvi, J.T., Kasa, S., Pakkanen, T.A. (2019). Influence of temperature on the swelling pressure of bentonite clay. Chemical Physics, 516, 177-181.

Cui, S.L., Du, Y.F., Wang, X.P., Huang, S., & Xie, W.L. 2018. Influence of temperature on swelling deformation characteristic of compacted GMZ bentonite-sand mixtures. J. Cent. South Univ. 25: 2819−2830.

Komine H., Yasuhara K., and Murakami S. 2009. Swelling characteristic of bentonite in artificial seawater, Canadian Geotechnical Journal, 46, 177-189.

Lin, L. C., & Benson, C. H. 2000. Effect of wet-dry cycling on swelling and hydraulic conductivity of GCLs. Journal of Geotechnical and Geoenvironmental Engineering, 126 (1), 40-49.

Liu, L. N., Chen, Y. G., Ye, W. M., Cui, Y. J., & Wu, D. B. 2018. Effects of hyperalkaline solutions on the swelling pressure of compacted Gaomiaozi (GMZ) bentonite from the viewpoint of Na+ cations and OH–anions. Applied Clay Science, 161, 334-342.

Mašín, D. 2005. A hypoplastic constitutive model for clays. International journal for numerical and analytical methods in geomechanics, 29, 311-336.

Mašín, D. 2013. Double structure hydromechanical coupling formalism and a model for unsaturated expansive clays. Engineering Geology, 165, 73-88.

Mašín, D. 2017. Coupled thermohydromechanical double-structure model for expansive soils. Journal of Engineering Mechanics, 143 (9), 04017067.

Schanz, T., & Al-Badran, Y. 2014. Swelling pressure characteristics of compacted Chinese Gaomiaozi bentonite GMZ01. Soils and Foundations, 54 (4), 748-759.

Shirazi SM, Kazama H, Chim-oye W and Kuwano J. 2008. Effect of void ratio on swelling and permeability of bentonite. Australian Geomechanics, 43 (2), 9-19.

Tang, C. S., Shi, B., Liu, C., Suo, W. B., & Gao, L. 2011. Experimental characterization of shrinkage and desiccation cracking in thin clay layer. Applied Clay Science, 52 (1-2), 69-77.

Zhu, C. M., Ye, W. M., Chen, Y. G., Chen, B., & Cui, Y. J. 2013. Influence of salt solutions on the swelling pressure and hydraulic conductivity of compacted GMZ01 bentonite. Engineering Geology, 166, 74-80.